NATIONAL AERONAUTICS AND SPACE ADMINISTRATION

Technical Memorandum 33-760

New Potentials for Conventional Aircraft When Powered by Hydrogen-Enriched Gasoline

Wesley A. Menard

Philip I. Moynihan

Jack H. Rupe

JET PROPULSION LABORATORY

CALIFORNIA INSTITUTE OF TECHNOLOGY

PASADENA, CALIFORNIA

January 15, 1976

PREFACE

The work described in this report was performed by the Propulsion Division of the Jet Propulsion Laboratory.

ACKNOWLEDGMENTS

The authors wish to acknowledge the valuable contributions made to this effort by several individuals at JPL and in industry. In particular, we wish to acknowledge the Analysis Task Team members, who were T. G. Vanderbrug, S. P. DeGrey, and R. K. Baerwald, Jr., and those who provided support to this activity: J. E. Chirivella, J. Foster, C. Peterson, and G. D. Anderson. Inputs from industry were invaluable to the study. Special recognition is due F. W. Riddell and L. Duke from AVCO Lycoming, who contributed to the engine analysis, and R. C. Umscheid of Beech Aircraft Corporation, who performed the turbocharged aircraft performance calculations.

CONTENTS

ABSTRACT

Hydrogen enrichment for aircraft piston engines is under study in a new NASA program. The objective of the program is to determine the feasibility of inflight injection of hydrogen in general aviation aircraft engines to reduce fuel consumption and to lower emission levels.

A catalytic hydrogen generator will be incorporated as part of the air induction system of a Lycoming turbocharged engine and will generate hydrogen by breaking down small amounts of the aviation gasoline used in the normal propulsion system. This hydrogen will then be mixed with gasoline and compressed air from the turbocharger before entering the engine combustion chamber. The special properties of the hydrogen-enriched gasoline allow the engine to operate at ultralean fuel/air ratios, resulting in higher efficiencies and hence less fuel consumption.

This paper summarizes the results of a systems analysis study. Calculations assuming a Beech Duke aircraft indicate that fuel savings on the order of 20% are possible. An estimate of the potential for the utilization of hydrogen enrichment to control exhaust emissions indicates that it may be possible to meet the 1979 Federal emission standards.

INTRODUCTION

The reduction of fuel consumption and of exhaust pollution are two of the most pressing problems facing the light aircraft industry today. This paper describes a technique by which improvements in both these problem areas are possible with a relatively small modification to aircraft piston engines. The concept takes advantage of the fact that the thermal efficiency of internal combustion piston engines improves [1] with lean combustion. By mixing hydrogen with the normal gasoline fuel, the lean flammability limit of the fuel is extended to ultralean fuel/air mixtures, allowing the engine to benefit from the improved thermal efficiency. The practicality of the concept is further enhanced by catalytically generating the hydrogen from gasoline on the aircraft. Hydrogen is generated and consumed as required by the engine, eliminating possible safety and logistics problems which may be associated with carrying gaseous or liquid hydrogen on board. Recent laboratory experiments with a single-cylinder research engine and V-8 automobile engines at JPL [2-4] have demonstrated substantial improvements in thermal efficiencies and reduction in NO_x emissions with the hydrogen enrichment concept. An aircraft engine should respond in a similar manner. In order to investigate to what extent it will respond, the present NASA-sponsored research and development program was undertaken.

The research is being conducted in three phases. Phase I involved a systems analysis of the integrated hydrogen generator, engine, and aircraft system. In Phase II the predictions of the systems analysis will be verified in the laboratory through engine/hydrogen generator dynamometer experiments. The Phase III effort will involve flight-testing to verify the laboratory results and to investigate altitude- and aircraft-related effects.

This paper reports the results of the Phase I systems analysis study. The objective of the study was to determine the feasibility of the hydrogen enrichment concept by characterizing the overall system efficiency and aircraft performance. This was accomplished by formulating analytical representations of an aircraft piston engine system, including all essential components required for onboard hydrogen generation. To assist in the study, the services of AVCO Lycoming, a major manufacturer of aircraft piston engines, and Beech Aircraft, a major assembler of general aviation aircraft, were obtained through contracts with JPL. The analysis contained herein was therefore a combined JPL-industry effort. JPL developed the analytical modeling of the problem and calculated the operational characteristics of the integrated generator/engine system; Lycoming determined the critical altitude; and Beech computed the aircraft performance.

SYSTEM DESCRIPTION

The aircraft being used in the program is a Beech Model 60 Duke. A photograph of the airplane in flight is shown in FIG. 1. The airplane has a gross weight of 6775 lb, can cruise at 250 mph at an altitude of 25,000 ft, and has a range in excess of 1000 miles. The twin-engine Beech Duke was selected because it is large enough to accommodate flight test equipment and crew during the experimental phase of the program, it has high-altitude capability and good engine performance, and it is generally representative of modern general aviation technology.

Power is supplied by two direct-drive, 541-in.^{3}-displacement Lycoming engines. A top view of an "F" model engine is shown in FIG. 2. The turbocharged, fuel-injected engine develops 380 horsepower at 2900 rpm. It is air-cooled, has six horizontally opposed cylinders, and uses 100/130 octane aviation grade gasoline. The compression ratio is a relatively low 7.30:1.

The third major component to be considered in the systems analysis is the hydrogen generator. The generator is an additional component mounted on the engine. A portion of the gasoline flowing to the engine will be diverted to the generator, where it will be catalytically reacted to produce a hydrogen-rich gas. A cutaway view of a hydrogen generator designed at JPL for an automotive application is shown in FIG. 3. The aircraft design will be functionally similar to the one shown. During steady-state operation, fuel and air enter the generator, where they are heated and mixed. Next, they are passed into the hot catalyst bed, where they are decomposed by the process of partial oxidation, forming a hydrogen-rich product gas. To maximize hydrogen yield, the hydrogen generator is run with a rich fuel/air mixture [5]. The optimum generator equivalence ratio for hydrogen generation has been found to be 2.75. At this condition the generator produces a product gas consisting of 21% H_2, 23% CO, 52% N_2, and 4% other species (by volume). A more complete listing of the product composition is shown in FIG. 4. The hydrogen produced as a function of input fuel flow rate is also shown. Measurements at the lower flow rates (< 18 lbm fuel/hr) have shown that the variation of hydrogen produced is very nearly linear with fuel input, and that the variation in composition of the combustibles is small [6]. As seen in the figure, approximately 8.5 lbm of fuel is consumed in the generation of 1 lbm of hydrogen.

Integration of the hydrogen generator with the engine is illustrated schematically in the simplified flow diagram of FIG. 5. In normal operation the engine receives air from the compressor side of the turbocharger and fuel from the fuel tank. Power is produced and the exhaust gases are used to drive the turbine side of the turbocharger. The wastegage valve controls the turbine speed by varying the exhaust flow to the turbine. When the hydrogen generator is added, the flow diagram is modified as indicated by the dashed lines. Some of the fuel and air are now diverted to the generator to produce the hydrogen-rich product gas. To maintain high volumetric efficiency and to avoid material fatigue within the air induction system, an air/gas heat exchanger reduces the 1800°F product gas temperature to 500°F. In the analysis, the thermodynamic state conditions were computed throughout the flow system to determine the impact of adding the hydrogen generator. For instance, if the pressure drop through the generator and heat exchanger exceeded 3 psi, an additional pump would be required in the system to recover the lost pressure. Also, the energy availability of the exhaust gas must be sufficient so that the turbocharger can supply an adequate intake manifold pressure.

For the analysis it was assumed that the hydrogen generator would be installed directly on top of the engine and contained within the engine's modified air induction system. The modified induction system would be larger than the one in the standard engine and would require an aerodynamic blister located on the top of the cowling. A preliminary installation drawing of this configuration, prepared by Beech Aircraft Corporation, is presented in FIG. 6. The increased nacelle aerodynamic drag, as well as the additional

weight for the hydrogen generator on each engine, was included in the aircraft performance calculations.

ENGINE ANALYSIS

To study the performance and fuel consumption characteristics of the engine/hydrogen generator system, the brake horsepower (BHP) and brake specific fuel consumption (BSFC) were determined for various operating conditions. The engine speed, operating altitude, intake manifold pressure, and hydrogen flow rate were selected as independent variables, and a parametric study was conducted. Wherever possible, empirical data were utilized.

The brake horsepower is defined as

$$BHP = IHP - FHP \tag{1}$$

where IHP is the indicated horsepower and FHP is the friction horsepower, which is known for the Lycoming engine as a function of rpm. The indicated horsepower is expressed as follows:

$$IHP = \frac{\eta_t}{J}\left[\left(\dot{m}_{g(eng)}\ h_g\right) + \Sigma(\dot{m}_i\ h_i)\right] \tag{2}$$

where η_t is the engine indicated thermal efficiency, J is Joule's law coefficient (J = 2545 Btu/IHP - hr), $\dot{m}_{g(eng)}$ is the mass of gasoline supplied to the engine per unit time, and h_g is heat of combustion of a unit mass of gasoline. The summation terms account for the energy content of the combustible species produced by the hydrogen generator per unit time. These include gaseous H_2, CO, and CH_4, which flow to the engine as additional fuels. Gasoline consumed by the generator, $\dot{m}_{g(gen)}$, in the production of the hydrogen product gas is accounted for by defining the brake specific fuel consumption for the engine as

$$BSFC = \frac{\dot{m}_{g(eng)} + \dot{m}_{g(gen)}}{BHP} \tag{3}$$

Equations (1), (2), and (3) are the basic equations, and to solve them requires a knowledge of η_t and $\dot{m}_{g(eng)}$ as functions of the independent variables. It will shown later (in FIG. 7) that the thermal efficiency depends upon the hydrogen mass flow rate to the engine, the engine speed, the manifold pressure, and the equivalence ratio. In functional form,

$$\eta_t = f_1(\dot{m}_{H_2},\ RPM,\ P_{man},\ \phi) \tag{4}$$

The equivalence ratio is a normalized fuel-to-air ratio,

$$\phi = \frac{(\dot{m}_f/\dot{m}_a)_{ACTUAL}}{(\dot{m}_f/\dot{m}_a)_{STOICH}} \tag{5a}$$

where $(\dot{m}_f/\dot{m}_a)_{ACTUAL}$ is the ratio of the actual fuel and air consumed by

the engine, and $(\dot{m}_f/\dot{m}_a)_{STOICH}$ is the stoichiometric ratio. For a given mass flow rate of fuel the equation can be simplified to

$$\phi = \frac{\dot{m}_{a,ST}}{\dot{m}_{a,AC}} \tag{5b}$$

Separating $\dot{m}_{a,ST}$ into components for each of the combustible fuel species gives

$$\phi = \frac{\dot{m}_{a(g),ST} + \dot{m}_{a(H_2),ST} + \dot{m}_{a(CO),ST} + \dot{m}_{a(CH_4),ST}}{\dot{m}_{a(eng)}} \tag{5c}$$

The terms in the numerator are the stoichiometric mass flow rates of air for gasoline, hydrogen, carbon monoxide, and methane. In the denominator, $\dot{m}_{a(eng)}$ is the actual air flow to the engine. The hydrogen generator products and the required stoichiometric air are known quantities once the desired hydrogen flow rate, $\dot{m}_{H_2}$, is selected (see FIG. 4). The stoichiometric mass flow rate of air for gasoline depends upon the gasoline flow, so the only other remaining unknown in (5c) is $\dot{m}_{a(eng)}$.

The gasoline flow rate to the engine may also be written in terms of $\dot{m}_{a(eng)}$ [7]:

$$\dot{m}_{g(eng)} = \zeta_g \left[\phi\left(\dot{m}_{a(eng)} + \dot{m}_{dil}\right) - \dot{m}_{a(p),ST}\right] \tag{6}$$

where ζ_g is the stoichiometric fuel/air ratio for gasoline, $\dot{m}_{dil}$ is the diluent mass flow rate, and $\dot{m}_{a(p),ST}$ is the stoichiometric air for the generator product gas. Therefore, BHP and BSFC can be computed once $\dot{m}_{a(eng)}$ is determined, which is accomplished by simultaneous solution of the following three equations:

$$\dot{m}_{a(eng)} = \eta_V \frac{RPM}{C_1} V \frac{P_{man}}{T_{mix}} - C_2 \frac{\dot{m}_p}{\bar{M}} \tag{7}$$

$$\eta_V = f_2\left(P_{man},\ T_{mix},\ \phi,\ RPM\right) \tag{8}$$

$$T_{mix} = \frac{\dot{m}_{a(eng)}\ c_{p(a)}\ T_c + \dot{m}_p\ c_{p(p)}\ T_{gen}}{\dot{m}_{a(eng)}\ c_{p(a)} + \dot{m}_p\ c_{p(p)}} \tag{9}$$

where η_V is the volumetric efficiency, shown in functional form, and T_{mix} is the temperature of the mixed induction air and generator product gases. The other parameters introduced are the constants C_1 and C_2, engine displacement V, product gas mass flow rate $\dot{m}_p$, mean molecular weight $\bar{M}$, the specific heats of air and product gas $c_{p(a)}$ and $c_{p(p)}$, and the turbocharger compressor

discharge temperature T_c. The volumetric efficiency was estimated empirically from Lycoming engine performance measurements.

To facilitate the parametric study, a computer program was written to solve the above equations. It also computed the thermodynamic conditions and pressure losses throughout the flow system and iterated an energy balance between the turbocharger compressor demand and the energy supplied by the turbine. In the turbocharger calculation a knowledge of the exhaust gas energy available to drive the turbine is required. Much of this information was obtained from Lycoming exhaust gas temperature measurements, but for lean mixtures and high engine power conditions such data are not available. The maximum allowable turbine inlet temperature is approximately 1650°F, so the engine cannot be operated at conditions where this "red line" is exceeded. With hydrogen enrichment, leaning to lower ϕ is possible and lower exhaust gas temperature results. An estimate of the exhaust gas energy available to the turbine at these operating conditions was therefore made on the basis of automobile engine measurements. More details of the analysis techniques, computer program, and assumptions used are given in a JPL internal document of the Phase I study (Ref. 8).

The most important input required for the solution of Eq. (1)-(3) is the engine thermal efficiency. The effect of hydrogen enrichment on η_t is not known for certain since the engine has never been tested for this effect. But we can draw upon previous experience at JPL in applying the hydrogen enrichment concept to other internal combustion engines.

In FIG. 7, thermal efficiency measurements for a 350-in.^{3} Chevrolet V-8 engine are shown as a function of ϕ for various hydrogen enrichments. Two sets of data are presented. The open symbols are for 2000 rpm and 40 bhp, simulating a vehicle road load speed of about 55 mph. The closed symbols are for a higher engine speed and load condition. As was mentioned previously, one can see that, as the amount of hydrogen in the fuel is increased from 0 to 1.0 lbm H_2/hr, (1) the thermal efficiency curves are extended to leaner equivalence ratios, and (2) the peaks of the η_t curves increase. Note that for one engine condition when hydrogen was added there was an immediate "jump" in η_t even before leaning out, whereas in the other condition no such jump occurred. At this time we have no satisfactory explanation for these observations. The band shown in the figure represents sea-level aircraft engine data for a speed range of 2300-2750 rpm and a range in manifold pressure from 28 to 44 in. Hg. In the ϕ region where the automobile and aircraft data overlap, the thermal efficiency of each engine is approximately the same. Therefore, in the system analysis the aircraft thermal efficiency for lean equivalence ratios ($\phi < 1.0$) was estimated by following the trends of the car data. However, since the car showed a jump at one condition and not at another, we assumed both possibilities for the aircraft engine in the calculations. As indicated in Eq. (4), the thermal efficiency is also a function of rpm and P_{man}. Relatively small adjustments were applied to the η_t curves of FIG. 7 to account for variations of these parameters.

Using the above analysis techniques, engine performance was calculated for a wide range of operating conditions and hydrogen flow rates. Typical results of these calculations are presented in FIGS. 8-11.

In FIG. 8, brake specific fuel consumption for 2-lbm/hr hydrogen enrichment is compared with the gasoline-only case for an engine running at 2600 rpm,

36 in. Hg manifold pressure, and 20,000-ft altitude. The two solid curves are for the two η_t assumptions described above. Also shown are actual Lycoming measured data points. Agreement with the calculated gasoline-only curve tends to verify the analysis techniques. For cooling purposes, the engine presently operates with rich fuel/air mixtures. For instance, $\phi = 1.1$ may be a typical cruise setting, and $\phi = 1.4$ is typical for climb. During takeoff, the fuel/air mixture is even richer. With the hydrogen-enriched engine it is planned to operate at $\phi < 0.9$, so the anticipated improvement will come by moving from a rich operating condition, $\phi > 1.1$, to a lean one. Which thermal efficiency assumption applies below $\phi = 0.9$ has less significance in improved BSFC than does the effect of moving from the rich ϕ regime.

The following comparative examples will therefore be simplified by presenting only the results for the η_t assumption (nonconservative) based on the low-power automotive measurements in FIG. 7.

The power produced for the above example is shown in FIG. 9. Here the brake horsepower is shown as a function of ϕ for 0, 1, 2, and 3 lbm H_2/hr. The lean flammability limit for each fuel mixture is indicated. The gasoline-only lean limit represents test stand data and not the practical operating condition which is again at $\phi > 1.1$. Note that as the engine is leaned out, a constant power requirement can be satisfied beyond the gasoline-only curve by enriching with hydrogen. This is the case for all power settings except those near maximum. The engine's maximum rated horsepower cannot be obtained with the hydrogen generator installed and operating in the system. The generator has a fuel conversion efficiency of 80%, and under full load conditions the gasoline consumed by the generator could be more effectively used if consumed directly by the engine to produce power.

FIG. 10 is a typical altitude performance map. It shows brake horsepower developed with different manifold pressures as a function of altitude. The map is for a hydrogen enrichment of 2 lbm/hr and a constant BSFC of 0.3893 lbm/hp-hr. The power setting is 75%, or 285 hp. At low altitudes this power can be obtained with any of the pressures shown. As altitude is increased, however, higher manifold pressures are required. When the turbocharger can no longer supply higher pressures, a critical altitude is reached for that power setting. For this example, the critical altitude is between 25,000 and 26,000 ft. The critical altitude for the standard engine is 30,000 ft, indicating that the hydrogen generator penalizes the altitude performance for this power setting by about 5000 ft.

The optimum hydrogen flow rate for the system is shown in FIG. 11. Here, brake specific fuel consumption vs hydrogen mass flow rate is plotted for two power settings. The best fuel economy occurs at 1.5 lbm H_2/hr. Calculations for other engine operating conditions yield similar results. Measurements of the actual engine operating conditions are shown for comparison.

AIRCRAFT PERFORMANCE

To determine the aircraft performance the installed power of the engine must be computed. This was done using a Beech computer program which corrects engine performance maps (FIG. 10) for installation losses. The program accounts for the inlet temperature rise, accessory power, and engine cooling drag. It also calculates the propeller efficiency for each specific flight

condition. The resulting data were then used in another Beech program which combines the engine and aircraft characteristics and calculates the aircraft performance. In these calculations, consideration is given to the aircraft weight, aerodynamics, and fuel load.

A given flight may be separated into four primary parts: takeoff, climb, cruise, and descent. There will be no hydrogen enrichment during takeoff since this is a maximum power condition and should not be compromised in any way. However, substantial fuel savings may be obtained during climb, as shown for a typical flight in FIG. 12. Time to climb, fuel to climb, and distance traveled in climbing to any altitude are shown for the standard aircraft and for the hydrogen-enriched aircraft. During climb, the engine operates at 85% power and 2750 rpm. The intake manifold pressure is held at 36 in. Hg up to critical altitude, then increased to full throttle. An air speed of 161 mph is maintained up to 20,000 ft, and then the speed is decreased to 150 mph in climbing on up to 25,000 ft. In order to have a fair comparison between the two aircraft, their gross weights were fixed at 6775 lbm. The weight of two generators and associated hardware was assumed to be 88 lbm, so to maintain a constant vehicle weight the fuel supply in the hydrogen-enriched aircraft was reduced by an amount equivalent to the weight of the hydrogen generator system. The standard aircraft therefore retains its normal 202-gallon usable fuel capacity rating, while the hydrogen-enriched aircraft is given only a 187-gallon useble fuel supply. The hydrogen-enriched aircraft benefits from improved fuel economy but is also penalized for the additional weight of the system.

For a specific example, consider a climb to 25,000 ft. The standard aircraft consumes 215 lbm of fuel in climbing to altitude, while the hydrogen-enriched aircraft consumes only 131 lbm. This is a savings of 39%, and is a direct result of running the engines much leaner with hydrogen enrichment than without. The time and distance traveled in climbing to 25,000 ft are also reduced a small amount (approximately 3%) because of reduced cooling drag. The hydrogen-enriched engines run cooler, and the cowling flaps, which are opened into the free stream to draw air across the cylinders, need not be opened so far.

A comparative example for level cruise at 25,000 ft is presented in FIG. 13. Specific range (distance traveled/quantity of fuel consumed) for the standard aircraft and the hydrogen-enriched aircraft is plotted vs airspeed for several power settings. Improvements of 15% to 20% are typical for the hydrogen-enriched over the standard aircraft.

Integration of the aircraft performance characteristics over a given flight envelope is made to obtain a "range profile." The range profile is a plot of an airplane's flight path in altitude and range, where an accounting is kept of the fuel consumed along the path. One such profile is shown in FIG. 14 for an engine speed of 2750 rpm and a hydrogen flow rate of 1.5 lbm/hr. The aircraft starts, warms up, taxis out to the runway, takes off, climbs at 85% power to a desired altitude, then levels off to cruise at 75% power (for this example). Later it descends and shuts down. A typical short flight might be one where upon landing the standard aircraft has used 100 gallons of fuel, and a long flight might be one in which twice that amount of fuel is used. By enriching with hydrogen, the short flight could be made with only 76 gallons, for a savings of 24%. Likewise, the long-range flight would be made on 160 gallons. The dashed lines show how the

range could be extended. On a short-range flight the hydrogen-enriched airplane could fly approximately 175 miles farther than the standard airplane on 100 gallons of gasoline. Significant increases in range for longer flights are also predicted. Range profile calculations for a number of other engine power and speed conditions were performed and similar results were obtained [8]. It is appropriate here to comment on the effect of the thermal efficiency assumption used on the aircraft performance comparisons. If the conservative η_t assumption is made (see FIG. 8), the 39% fuel saving during climb would be reduced to 29%, and the 24% improvement in the range profile example would become 18%.

EXHAUST EMISSIONS

Emission standards for aircraft piston engines were promulgated by the Environmental Protection Agency and read into the Federal Register of July 17, 1973 [9]. Part 87.41 specifies that "Exhaust emissions from each new aircraft piston engine manufactured on or after December 13, 1979, shall not exceed:

(i) Hydrocarbons - 0.00190 pound/rated power/cycle

(ii) Carbon monoxide - 0.042 pound/rated power/cycle

(iii) Oxides of nitrogen - 0.0015 pound/rated power cycle"

These rules and regulations also specify the test procedures for engine operation (i.e., the 5-mode cycle intended to simulate aircraft operation) and the computation method to be used in determining mass emission rates. The latter includes a specification of time-in-mode (TIM). Thus it is possible to construct a table of "allowable" mass emission rates for any given engine for which the maximum rated horsepower and the manufacturer's recommended power settings for taxi, idle, and climbout are known.[1] TABLE I summarizes the allowable mass emission rates for the Lycoming TIO-541E engine and the work that must be done in each mode in order to complete one 5-mode cycle for this engine.

Although actual emission measurements are not available for the TIO-541E engine, an estimate of probable emission production can be derived if it is assumed that the "correlations" of emission production with ϕ as presented in FIGS. 15-17 are valid for that engine. The data base utilized in the development of these representations includes emission measurements reported by Requeriro [11] for a Continental IO-520-D aircraft engine and data obtained at JPL on the 350 CID V-8 automotive engine. In the latter case, data were obtained with both straight gasoline and mixtures of gasoline and the hydrogen-rich gases of a hydrogen generator [5]. Note that the correlations depend heavily on [11] for the rich data and on JPL-generated information for the lean region and that a reasonable coalescence occurs where these data sets join. We make no attempt to rationalize or justify the absolute magnitudes presented here and choose only to point out that

---

[1]Note: [9] specifies takeoff at 100%, approach at 40%, with climbout bounded by 75 and 100% of rated power; otherwise taxi/idle/climbout are at the manufacturer's recommended settings.

both qualitatively and quantitively the trends are consistent with most of the literature. For purposes of the comparison to be constructed here, the dominant effects are attributable to the ability to run an engine both efficiently and ultralean when hydrogen-enriched fuels are utilized. It should be obvious that substantial variations in quantitative values chosen for pollutant production will have only a small effect on the comparison. It may be pertinent to point out the following:

(1) The NO_x representation is an upper bound encompassing many different operating conditions for the V-8 (throttling, speed, load, etc.) and tends therefore to be conservative.

(2) The CO representation exhibits the rise to be expected from chemical equilibrium effects in the rich region and a contribution from the hydrogen generator that causes the rise in level for $\phi < 0.75$. Since no separation of CO production with H_2 fraction[2] was apparent, the upper bound on the region created by the V-8 data was used in the estimate involving hydrogen enrichment.

(3) The HC emission levels are inconsistent with theoretical considerations, but they are typical of measurements for IC engines. Hydrocarbon emissions are probably more engine-dependent than CO and NO_x. Levels chosen for the hydrogen-enriched case are for the upper bound of the V-8 operating region, which reflects an attempt to conservatively simulate the relatively low hydrogen concentration intended for the aircraft application.

TABLE II presents a comparison of emission characteristics to be expected for a standard engine and for one utilizing hydrogen enrichment. Note that the major change in operating conditions is in the equivalence ratio. For the lower power modes, hydrogen enrichment allows operation (still to be proven for the TIO-541) with ultralean mixtures and hence substantial changes in emission production rates relative to usual practice. In the illustration presented, climb power was reduced to the EPA-specified minimum in order to take advantage of a low ϕ operating condition for this mode. No change is allowed in the takeoff mode since this requires maximum horsepower available from the engine and cannot be compromised. However, this mode makes a relatively small contribution in either case to the total pollutant production.

In summary, it can be seen that the standard engine, when operated in the usual manner with relatively rich mixtures, is estimated to exceed the HC and CO standards by factors of 3 and 2, respectively, while the hydrogen-enriched configuration is estimated to yield only 0.64 and 0.08, respectivel of the allowable HC and CO standards. As indicated, we estimate that the NO_x yield, which is 0.26 of the emission Standard for the standard engine, will increase to 0.80 of the Standard when H_2 enrichment is applied. Obviously, experimental verification of these estimates is essential to the implementation of hydrogen enrichment for emission control purposes.

---

[2]Mass flow of H_2 per mass flow of all fuel species to the engine.

NATURALLY ASPIRATED AIRCRAFT

Naturally aspirated aircraft engines should also respond favorably to hydrogen enrichment. In fact, the only experimental measurements available using hydrogen enrichment are with naturally aspirated engines. The primary question to be answered in the aircraft application is how seriously the critical altitude is affected. As discussed previously, the hydrogen generator system reduces the maximum rated power of the engine. To what extent power is reduced was investigated through an analysis [8] assuming naturally aspirated Lycoming IO-540-K engines in the Beech Duke aircraft. They are similar to the standard Duke engines (TIO-541-E) with the exception of the turbocharger.

Some results from this analysis are presented in FIGS. 18 and 19. In FIG. 18, power and fuel consumption results are shown for an engine running both with gasoline only and with 1.5-lbm/hr H_2 enrichment. The calculations were performed for a typical cruise engine speed of 2600 rpm at an altitude of 5000 ft with wide-open throttle. The band for the hydrogen enrichment calculations represents the uncertainty due to the thermal efficiency assumption.

The BHP and BSFC curves show equivalence ratio trends similar to those shown in FIGS. 8 and 9 for the turbocharged engine. For a cruise setting of ϕ = 1.1, the engine produces a BSFC of 0.49 lbm/hp-hr on gasoline alone. An improvement of 8-18% is predicted by leaning out to ϕ = 0.80 with hydrogen enrichment. This is a significant fuel savings and is comparable to the turbocharged engine under the same conditions.

An estimate of the aircraft cruise performance at 2600 rpm and wide-open throttle as a function of altitude is shown in FIG. 19. As a point of reference, the available power and maximum cruise airspeed for gasoline only are shown as dashed curves. Power required for minimum control speed and for a constant 160-knot cruise velocity is also plotted. The reduced power from lean combustion results in lower obtainable airspeeds at all altitudes, but the percentage reduction becomes greater with increasing altitude. Critical altitude for gasoline only, at this operating condition, is 16,000 ft. With 1.5-lbm H_2/hr enrichment, critical altitude drops to approximately 14,000 ft. A loss of 2000 ft is not a severe penalty to pay for the significant improvements in fuel economy predicted. However, if higher-altitude capability is required for a particular flight plan (such as flying over the peaks of the Sierra Nevada mountain range) the pilot can, in principle, increase engine rpm or reduce hydrogen flow rate. The increased power obtained can be used to increase airspeed and consequently altitude. In this example the airplane can fly 1500 ft higher simply by increasing the engine speed by 150 rpm.

CONCLUSIONS

No major obstacles were encountered at the systems study level that prevent implementation of the hydrogen enrichment concept to aircraft piston engines. Relatively small quantities of hydrogen (1.5 lbm/hr) were found to yield significant improvements in fuel consumption on both turbocharged and naturally aspirated Lycoming 541-in.^{3} engines. Aircraft performance calculations predict fuel economy improvements up to 39% during climb and 20% in cruise, for an integrated range profile gain as high as 18-24%, depending upon the

engine thermal efficiency assumption. Operation of the hydrogen generator system will reduce critical altitude approximately 15%. The pilot can regain the lost altitude, however, by turning off the generator when desired. Exhaust emission estimates over the 5-mode Federal cycle suggest the possibility of meeting the Federal Standard with hydrogen enrichment. Emission levels are projected for NO_x, HC, and CO of 80%, 64%, and 8%, respectively, of those allowed by the Standard.

CONVERSION FACTORS FOR INTERNATIONAL SYSTEM UNITS

To convert from	to	multiply by
pound	kilogram	0.4536
inch	meter	0.0254
foot	meter	0.3048
mile (statute)	meter	1639
mile/hour	meter/second	0.4470
revolutions/minute	revolutions/second	0.01667
horsepower	watt	745.7
pound/hour	kilogram/second	0.000126
Fahrenheit	kelvin	$T_K = (5/9)(T_F + 459.7)$
inch of mercury	newton/meter^2	3386

REFERENCES

1. Taylor, C. F., and Taylor, E. S., The Internal Combustion Engine, Chapter 4, pp. 30-56, International Textbook Company, Scranton, Pa., 1950.

2. Breshears, R., Cotrill, H., and Rupe, J., "Partial Hydrogen Injection Into Internal Combustion Engine--Effect on Emissions and Fuel Economy," presented at the Environmental Protection Agency (EPA) First Symposium on Low-Pollution Power Systems Development, Ann Arbor, Mich., Oct. 14-19, 1973.

3. Hoehn, F. W., and Dowdy, M. W., "Feasibility Demonstration of a Road Vehicle Fueled With Hydrogen-Enriched Gasoline," Paper 749105, presented at the 9th Intersociety Energy Conversion Engineering Conference, San Francisco, Calif., August 26-30, 1974.

4. Hoehn, F. W., "Feasibility Demonstration of Hydrogen Enrichment Concept Using Experimental Catalytic Generator," IOM 38LPE-75-117, Jet Propulsion Laboratory, Pasadena, Calif., Oct. 8, 1974 (JPL internal document).

5. Houseman, J., and Cerini, D. J., "On-Board Hydrogen Generator for a Partial Hydrogen Injection Internal Combustion Engine," Paper 740600, Society of Automotive Engineers West Coast Meeting, Anaheim, Calif., Aug. 12-16, 1974.

6. "Hydrogen-Enrichment-Concept Preliminary Evaluation," Report 1200-237, Jet Propulsion Laboratory, Pasadena, Calif., July 1975 (JPL internal document).

7. Stocky, J. F., "An Estimate of the System Efficiency of the Hydrogen Injection Concept," IOM 38LPE-74-41, Jet Propulsion Laboratory, Pasadena, Calif., March 1974 (JPL internal document).

8. Moynihan, P. I., Menard, W. A., and Vanderbrug, T. G., "A Systems Analysis of Hydrogen-Enriched Fuel for General Aviation Aircraft," to be published as a JPL internal document, Jet Propulsion Laboratory, Pasadena, Calif.

9. Federal Register, Vol. 38, No. 136, p. 19088, July 17, 1973.

10. Syson, R. H., "Emission Characteristics of a Light Aircraft Piston Engine," presented at Society of Engineers Meeting, Wichita, Kan., Apr. 3, 1974.

11. Requeriro, J. F., Collection and Assessment of Aircraft Emissions, PB 204 196, Final Report to the Environmental Protection Agency, Teledyne Continental Motors, Oct. 1971.

TABLE I. EMISSION ALLOWABLES, MODE POWER,
AND MODE WORK FOR LYCOMING TIO-541 PISTON AIRCRAFT ENGINE

(Engine Rated Horsepower = 380 bhp at 2900 rpm.)

A. Maximum Allowed Emission Rate (Federal Standard)

Pollutant	Maximum Allowed			Average Rate Allowed, g/ihp-h
	lbm/rated power/cycle	g/rated power/cycle	g/cycle	
Hydrocarbons	0.00190	0.8618	327.48	5.12
Carbon Monoxide	0.0420	19.055	7240.9	113.3
Oxides of Nitrogen	0.0015	0.6804	258.6	4.05

B. Power Requirements by Operating Mode

Mode	RPM	BHP	FHP	IHP	Remarks
Maximum Power	2900	380	56	426	Maximum Rated Power
Idle	600	9	4.5	13.5	After Syson (Ref. 10)
Taxi	1200	30	11	43	After Syson (Ref. 10)
Approach	2750	152	50	202	40% Maximum Power; 2750 rpm
Climbout	2750	323	50	373	85% Maximum Power; 2750 rpm
Climb (Option)	2650	285	47	332	75% Maximum Power; EPA Minimum

TABLE I. (contd)

C. Work/Cycle by Operating Mode

Mode	Time in Mode, min	Work/Cycle,[a] ihp-h	Total Work in Mode, %
Taxi-Idle (Out)	12	8.11	12.69 13.41
Takeoff	0.3	2.13	3.33 3.52
Climbout	5.0 ---	31.08 ---	48.64 ---
Climb (Option)	--- 5.0	--- 27.67	--- 45.74
Approach	6.0	20.2	31.61 33.40
Taxi-Idle (In)	4.0	2.38	3.72 3.93
Total	27.3 27.3	63.90 60.49	99.99 100.00

[a]Taxi-idle mode is split as suggested by Syson (Ref. 10) to yield 1 min idle for each taxi-idle mode.

TABLE II. EMISSION ESTIMATE
FOR A TIO-541 ENGINE WITH AND WITHOUT HYDROGEN ENRICHMENT

A. Standard Engine

Mode	Air/ Fuel Ratio	ϕ	Emission Rate, g/ihp-h			Pollutant Produced, g		
			NO_x	HC	CO	NO_x	HC	CO
Taxi-Idle (Out)	8.7	1.66	.36	26	340	2.92	210.9	2757
Takeoff	10.6	1.36	2.3	3.1	120	4.90	6.6	256
Climbout (Rich)	10.4	1.39	1.9	3.5	135	52.6	96.8	3735
Approach	8.7	1.66	.36	26	340	7.21	520.5	6807
Taxi-Idle (In)	8.4	1.72	.25	70	400	.60	166.6	952
Total Pollutant Produced/Cycle, g						68.2	1001.4	14,507
Fraction of Allowable Standard						0.26	3.06	2.00

B. Engine With Hydrogen Enrichment

Mode	Air/ Fuel Ratio	ϕ	Emission Rate, g/ihp-h			Pollutant Produced per Mode, g		
			NO_x	HC	CO	NO_x	HC	CO
Taxi-Idle (Out)	24.1	0.6	1.2	4.0	7.4	9.73	32.4	60
Takeoff	10.6	1.36	2.3	3.1	120	4.90	3.1	256
Climb (Option)	20.6	0.7	6.0	3.0	4.5	166.0	83.0	125
Approach	24.1	0.6	1.2	4.0	7.4	24.0	80.1	148
Taxi-Idle (In)	24.1	0.6	1.2	4.0	7.4	2.9	9.5	18
Total Pollutant Produced/Cycle, g						207.5	208.1	607
Fraction of Allowable Standard						.80	.64	.08

FIG. 1. Beechcraft Duke B60

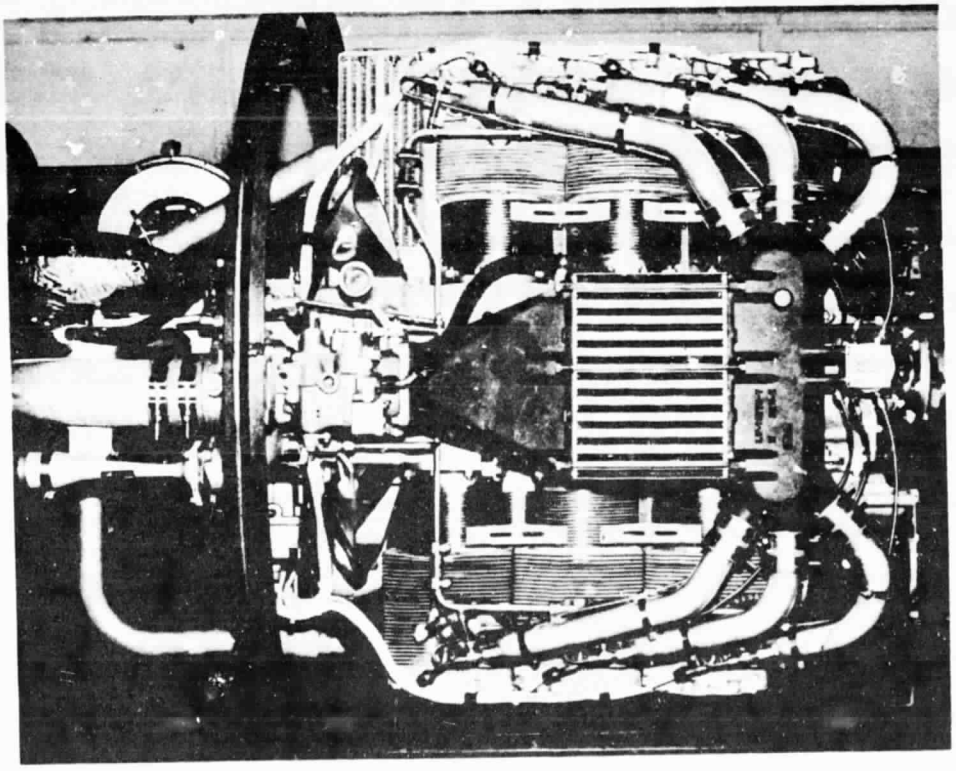

FIG. 2. AVCO Lycoming TIO-541F Engine

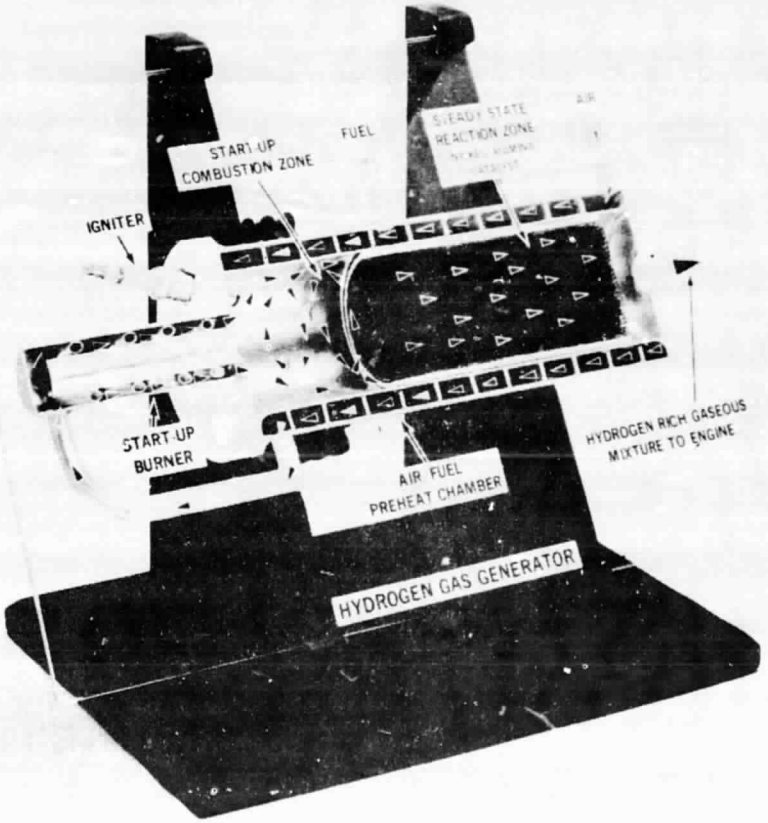

FIG. 3. Automotive Hydrogen Generator

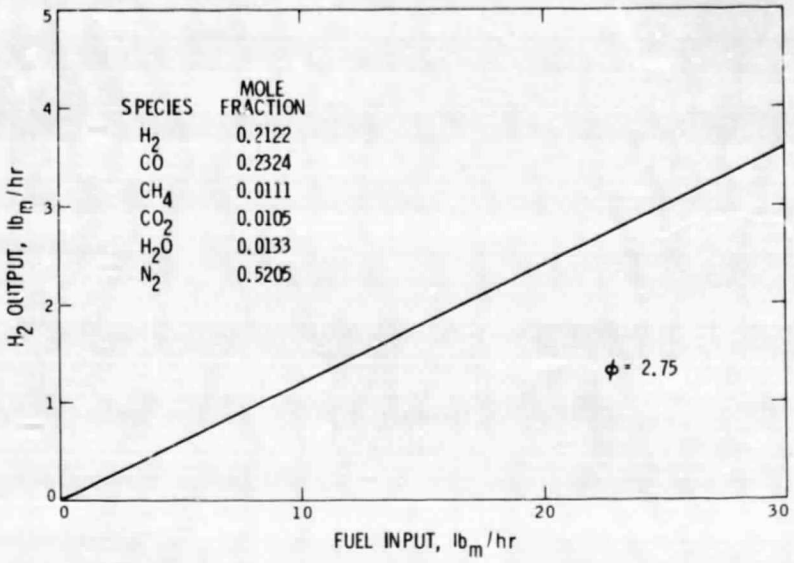

FIG. 4. Hydrogen Generator Product Gas

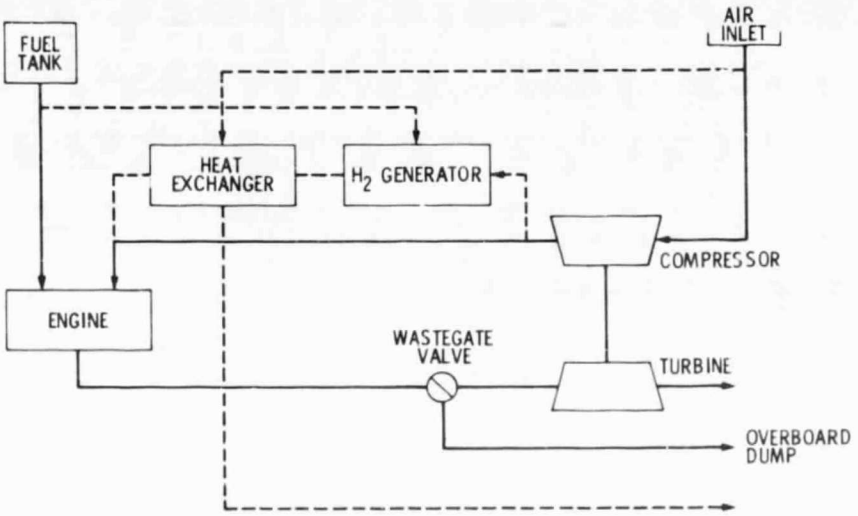

FIG. 5. Schematic Flow Diagram of Engine With Hydrogen Generator

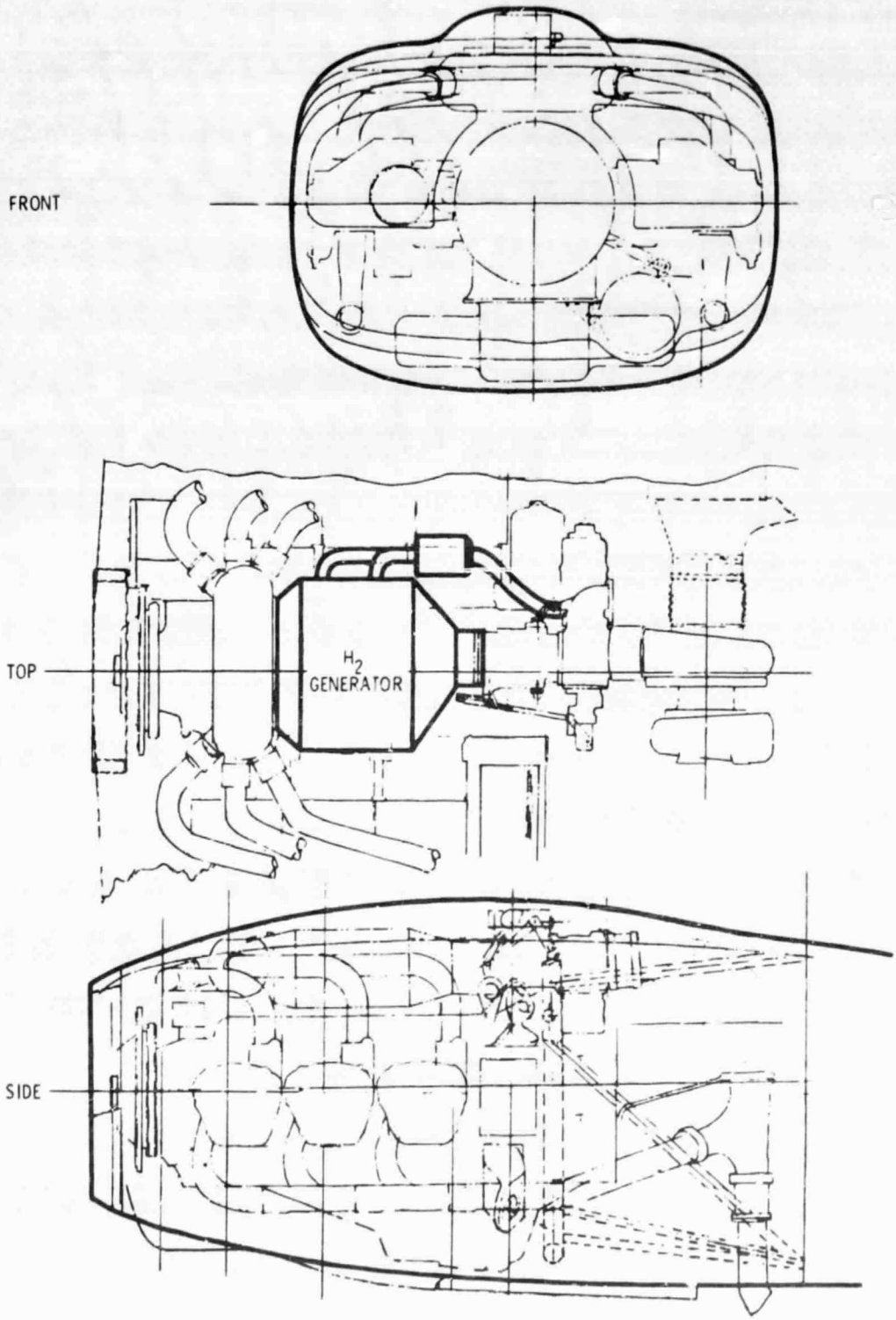

FIG. 6. Aircraft Installation of Hydrogen Generator (Preliminary Design)

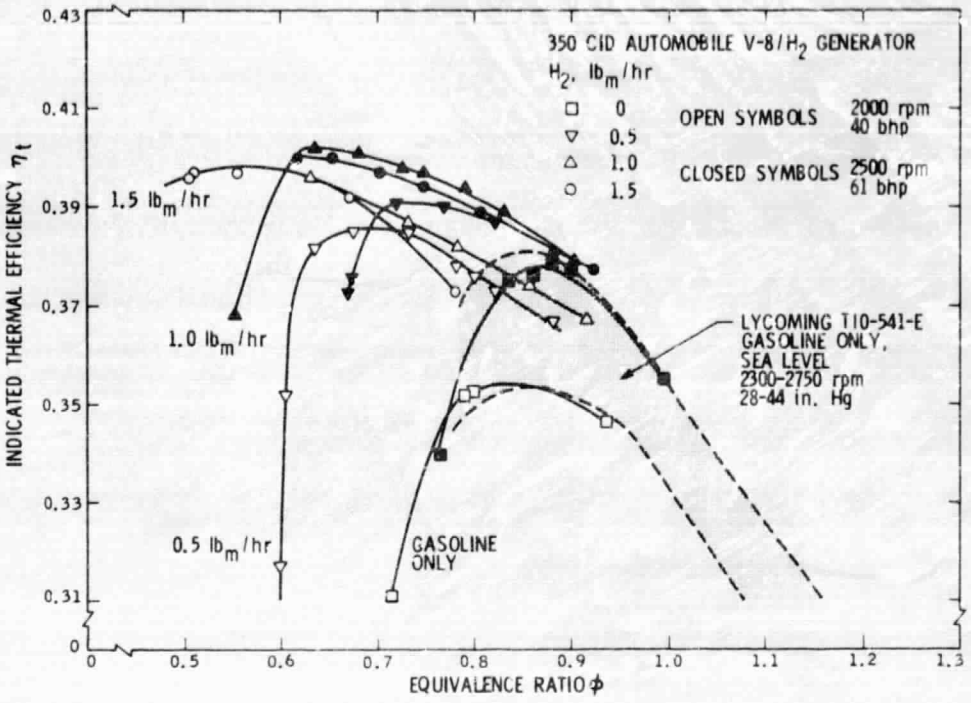

FIG. 7. Indicated Thermal Efficiency of Hydrogen-Enriched Engine

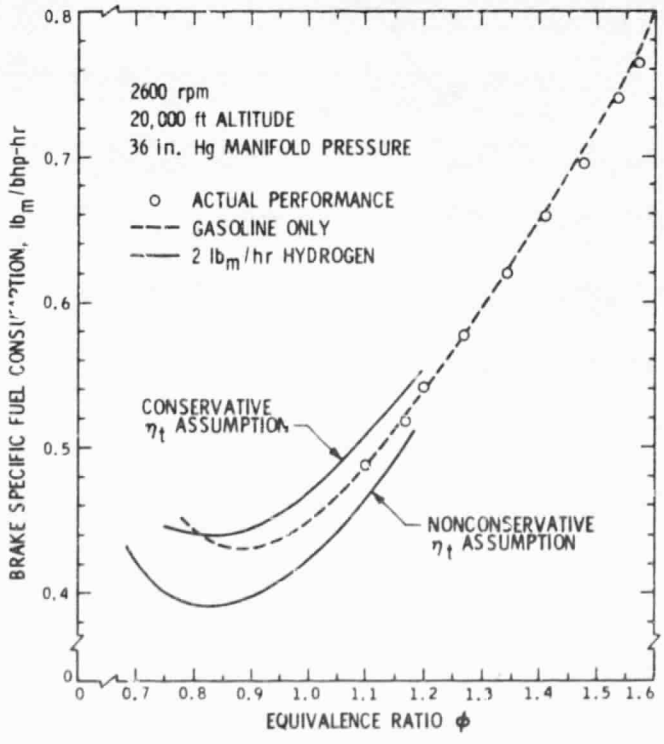

FIG. 8. Sample Results of Brake Specific Fuel Consumption, With and Without Hydrogen Enrichment

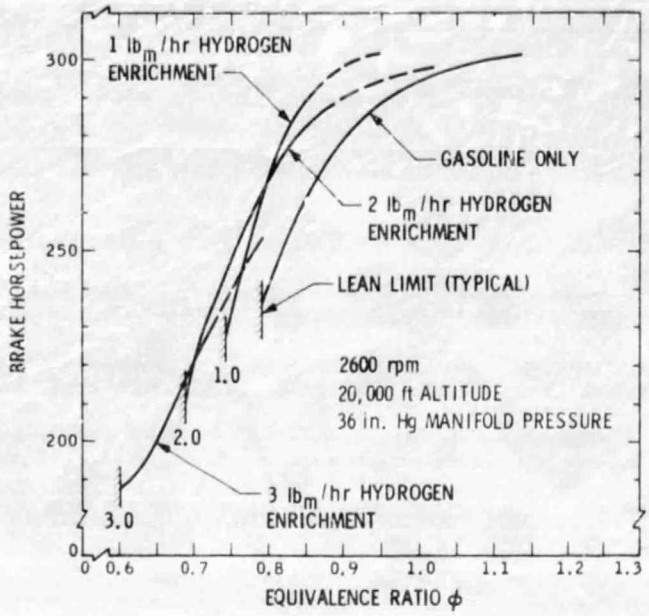

FIG. 9. Sample Results of Brake Horsepower, With and Without Hydrogen Enrichment

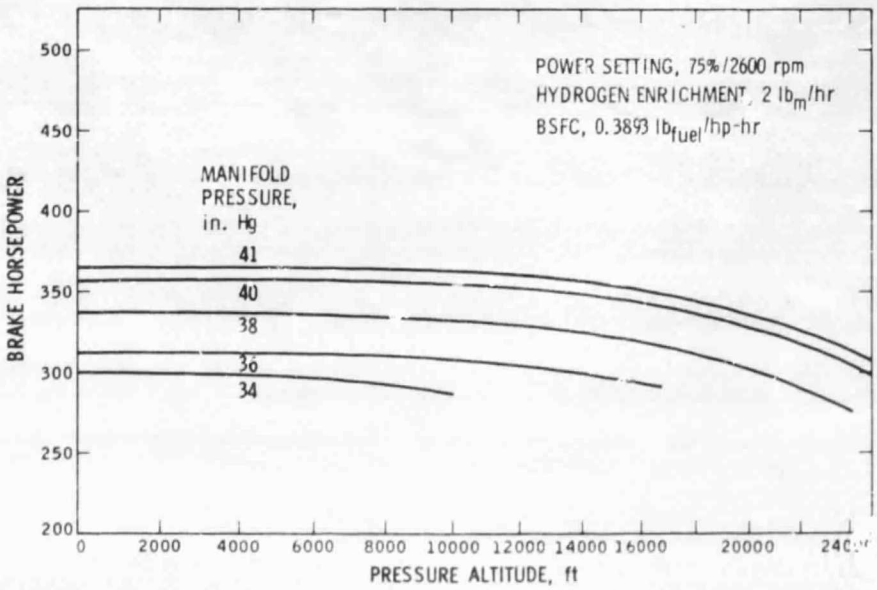

FIG. 10. Altitude Performance with Hydrogen Enrichment

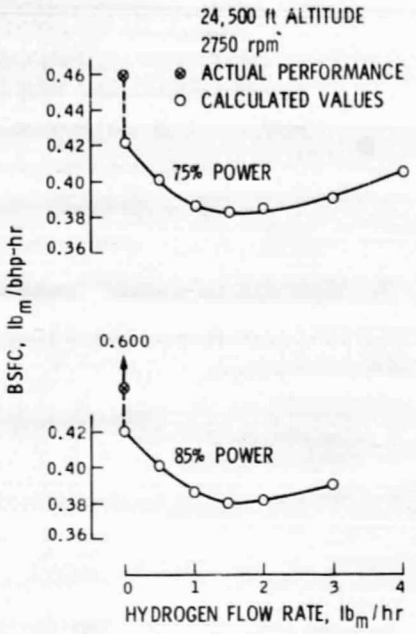

FIG. 11. Estimated Cruise Economy With Hydrogen Enrichment

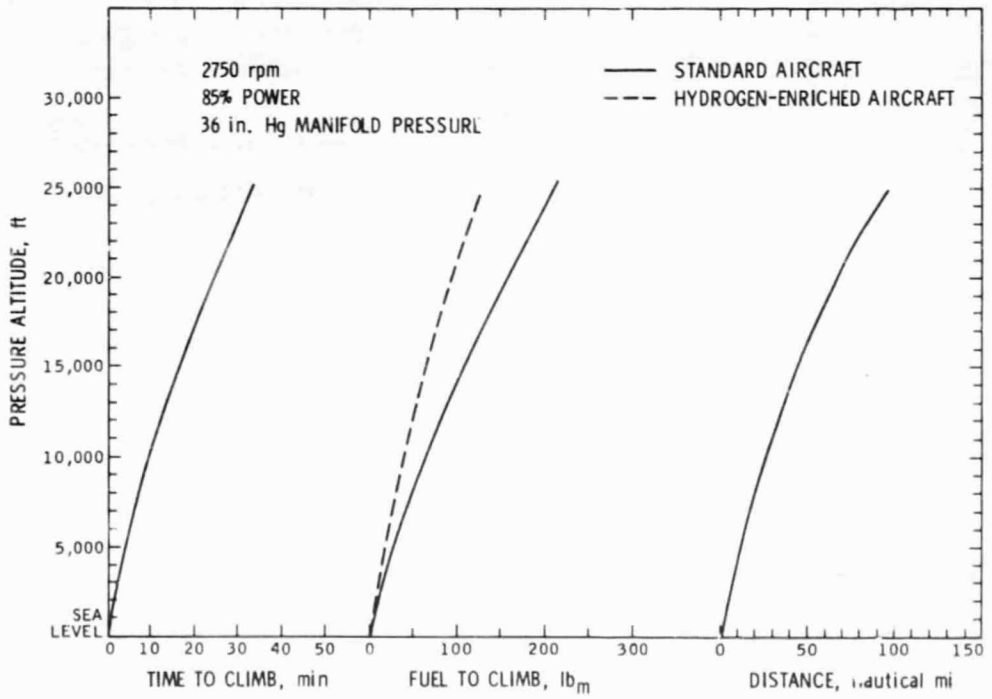

FIG. 12. Climb Comparison of Standard Aircraft to Aircraft With 1.5 lbm/hr Hydrogen

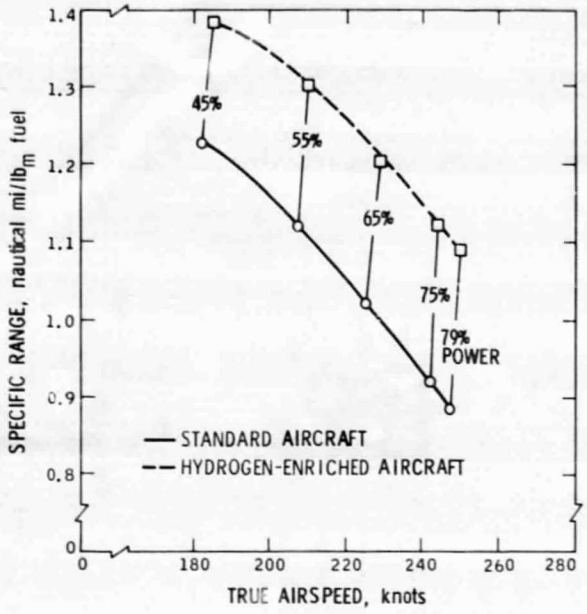

FIG. 13. Cruise Comparison of Standard Aircraft to Aircraft With 1.5 lbm/hr Hydrogen at 25,000 ft Altitude

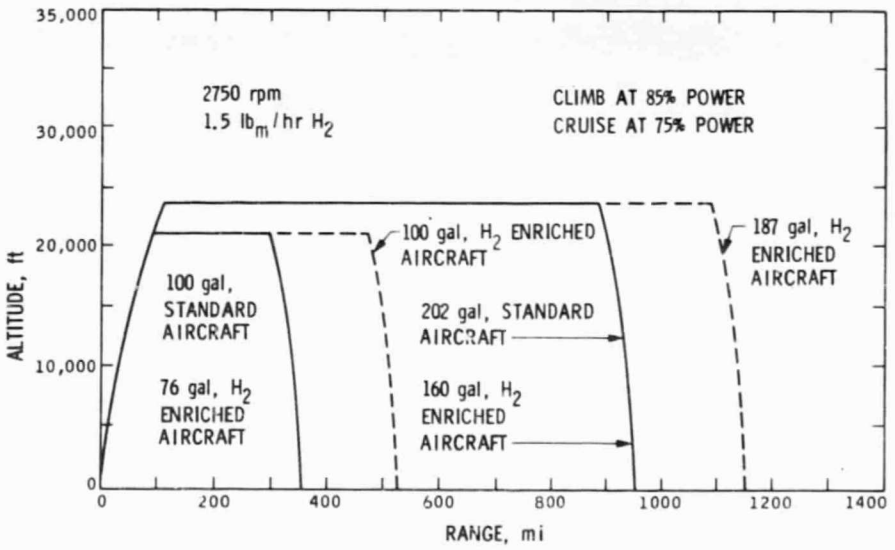

FIG. 14. Range Profiles With and Without Hydrogen Enrichment

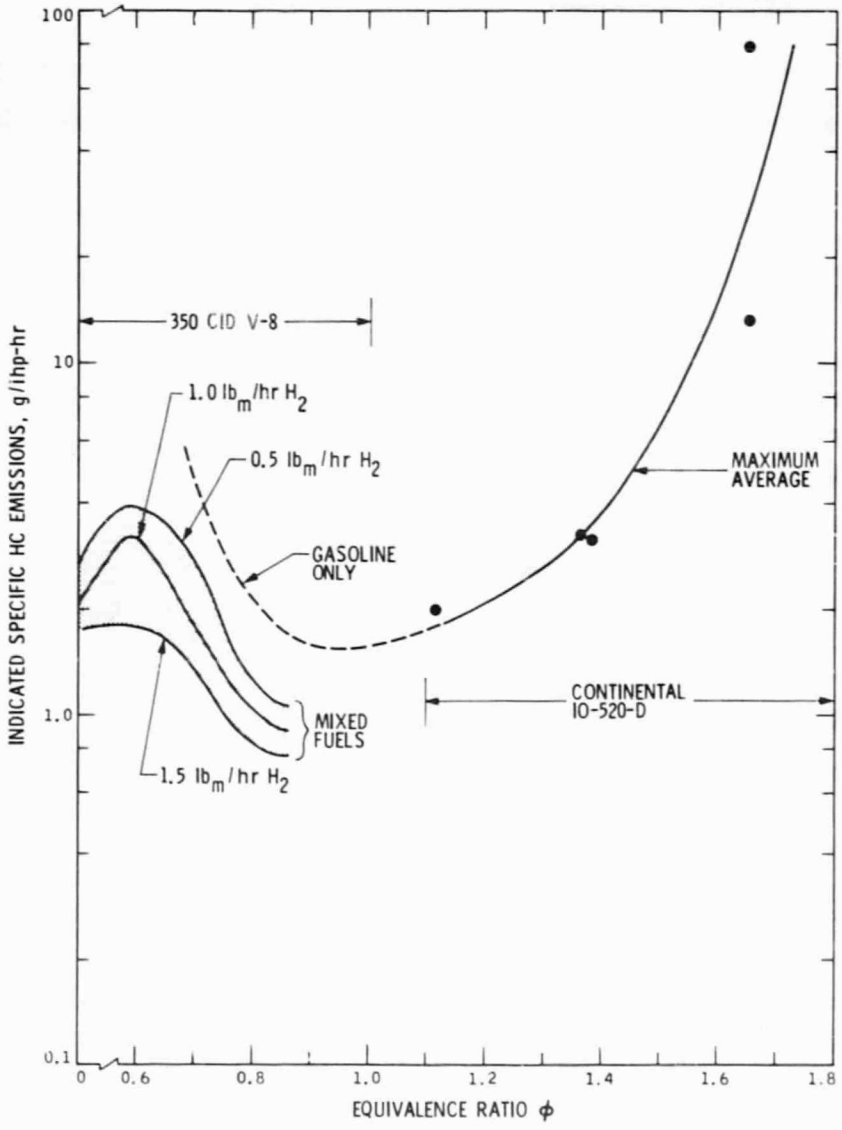

FIG. 15. Hydrocarbon Emission Rates for Spark Ignition Engines

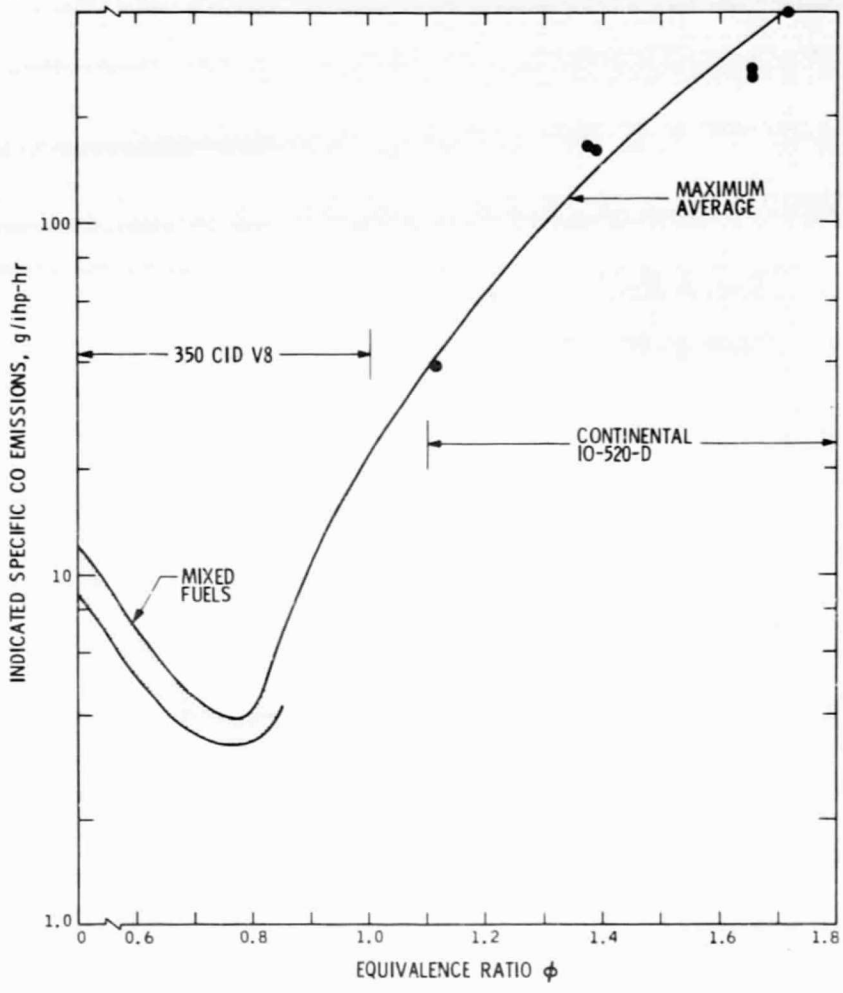

FIG. 16. Carbon Monoxide Emission Rates for Spark Ignition Engines

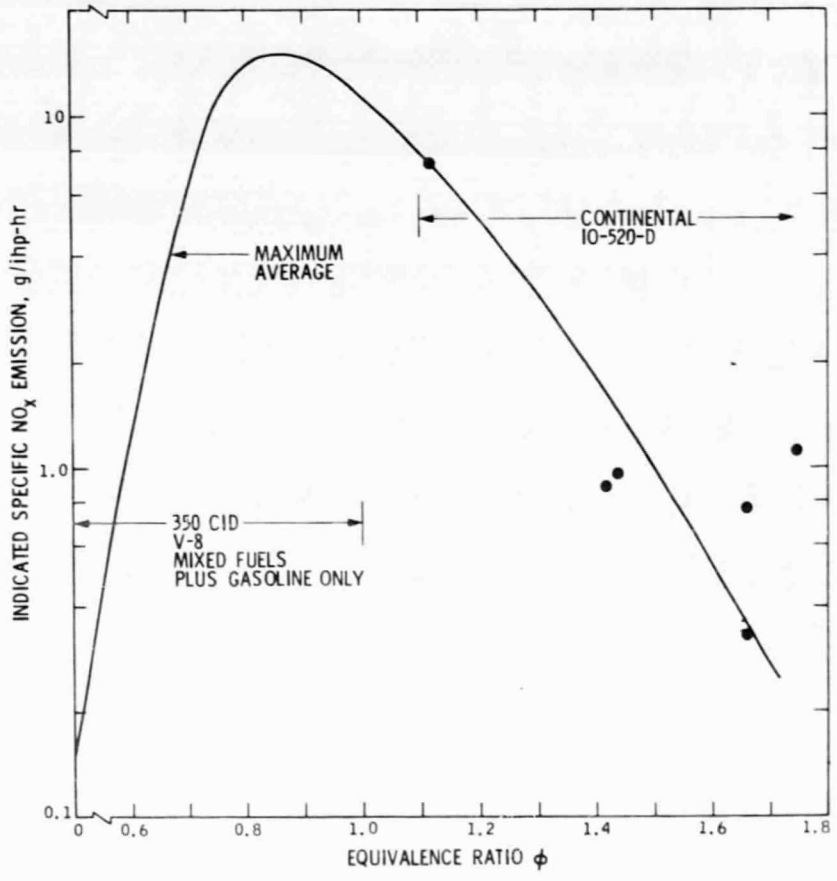

FIG. 17. Nitric Oxide Emission Rates for Spark Ignition Engines

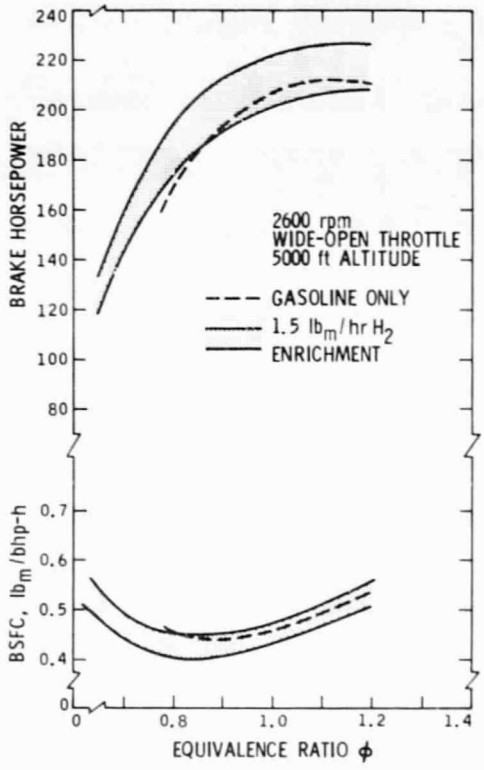

FIG. 18. Naturally Aspirated Engine Performance

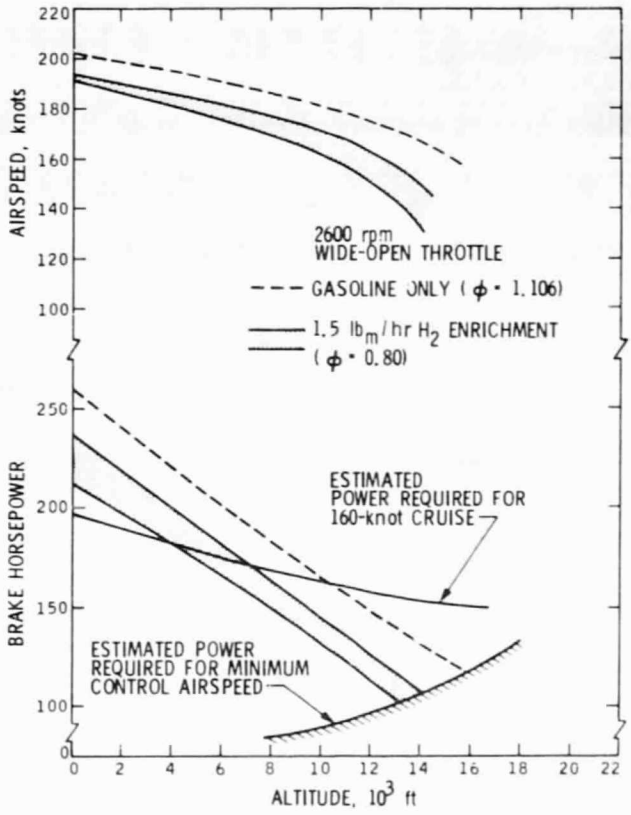

FIG. 19. Naturally Aspirated Aircraft Estimated Cruise Performance